Cervical image segmentation using active contours and evolutionary programming over temporary acetowhite patterns

Aldo Márquez-Grajales
Laboratorio Nacional de
Informática Avanzada, LANIA
Rébsamen 80, C.P. 91000 A.P. 696,
Col. Centro, Xalapa, Veracruz, México,
E-mail: li.aldomg@gmail.com

Hector-Gabriel Acosta-Mesa,
Efrén Mezura-Montes,
Artificial Intelligence Research Center
University of Veracruz,
Sebastián Camacho 5, Col. Centro.
Xalapa, Veracruz, México.
Email: heacosta@uv.mx, emezura@uv.mx

Rodolfo Hernández-Jiménez
Private Practice
Diego Leño 22,
Col. Centro, C.P. 91000,
Xalapa, Veracruz, México,
Email: roheji@msn.com

***Abstract*—Cervical Cytology or Pap Smear is the most popular technique for pre-diagnosis of cervical cancer. However, this technique has a high rate of false negative. As a consequence, it is necessary to complement it with other tests like Colposcopy. In some studies about the colposcopy test, it has been proposed that temporal changes intrinsic to the colposcopic image can be used to automatically characterize cervical lesions. In this document, a methodology to segment colposcopic images based on these temporal changes produced by the acetowhite reaction is presented in order to support to the colposcopist in the early detection of cervical cancer. This methodology consists in two stages: 1) a preprocessing stage, where several steps (extraction of time series, dimensionality reduction, classification process and a post-processing stage) are done to decrease problems or noise (specular reflection and keratosis) that can be seen as the acetowhite reaction, and 2) a segmentation stage where the active contour model (Snake) is used, changing the greedy search mechanism by a global search mechanism (evolutionary programming). The experiments were developed using only one colposcopic image and all the image sequence extracted from the colposcopy process. Results show that our methodology is a competitive tool to support to the colposcopist in the early detection of cervical cancer, providing one step towards the decrease of the mortality rate of this disease.**

I. Introduction

An estimated of 270000 female deaths in worldwide is presented due to the cervical cancer. Approximately, 85% of which occurs in developing countries [1]. In México 3840 deaths were reported by Globocan in its last statistics of 2012, representing a rate of 7.0 (estimated age-standardised rate) per 100000 women [2]. As a result, specialists perform several screening methods for early detection of cervical cancer. The Pap smear is the most common screening method used to detect abnormal cells on the cervix. However, this method suffers from several limitations, including sensitivity (generally, it is less than 50%) to detect cervical cancer precursors and the occurrence of false-negative [3]. Usually, a second test known as *Colposcopy* is performed to improve the Pap smear limitations.

Colposcopy consists in closer examination of the cervix by a magnifying instrument called Colposcope. Experts observe the reaction after applying dilute acetic acid on cervical epithelium. As a consequence, this application produces a temporary dehydration of the cytoplasmic womb. The acetic acid application on normal mature squamous epithelium does not have any effect. The epithelium absorbs the light and the specialist notes a pink or transparent tonality. Anomalous epithelial cells contain a large number of proteins. Thus, the acetic acid application produces a dehydration of hypertrophied nuclei. As a result, the light cannot pass through the epithelium, reflecting a white tone to the expert [4]. Colposcopists use this reaction to extract samples for biopsy test. However, other features as punctuate and mosaic patterns, are used by the specialists.

Despite the good results provided by the Colposcopy, it is considered a subjective test. In the first place, the diagnosis depends on specialist experiences and second, its interpretation could change in each expert [5]. In other words, the colposcopy accuracy is in function of physician training.

Costas J. Balas in [6] was one of the first researchers in to propose the use of spectroscopy to study the correlation between the acetowhite patterns and precancerous cervical lesions. His study demonstrated that the changes observed in the phenomenon are correlated with the type and degree of the cervical lesion.

Based on this correlation, some researchers have used the temporary patterns as a search guide to find precancerous cervical lesions in digital images. The main problem working with digital images is the presence of regions with tonalities similar to these patterns, such as specular reflection and keratosis that are not related to abnormal cell growth. We will refer to these characteristics as *noise*.

These studies were divided in two groups. In the first, works that used only one image to find the acetowhite reaction (static methods) were grouped. In this group we found to Van Raad et al. [7] who uses Gaussian pyramids and active contour model (Snake) to discriminate the noise and enclose the interest area, respectively; but even when acceptable results were achieved, the algorithm depended on the contour initialization and the selection of the image used for the different scales of the

pyramid. Another approach found in this block is presented by Nallaperumal et al. in [8], where the technique of *Watershed* or *line water division* is presented; this method consists in to obtain the gradients via multi-scale morphological operators and transforming the RGB color model (Red, green, blue) to the HSI model (Hue, Saturation, Intensity) because this model is related to human perception.

Finally, the second group contains those studies where the entire colposcopic image sequence is used. An example of this kind of researches is presented by Acosta et al. in [9], where a differentiation between the acetowhite patterns and noise was sought, calculating a minimum discriminator threshold and applying the Snake segmentation algorithm on the images; the main limitation of this study, as in [7], was the Snake contour initialization because the algorithm only seeks the interest zones in the internal areas of the contour, ignoring if the acetowhite reaction is present in external regions; that is, it presents a greedy behavior. In [10], a segmentation based on support vector machine (SVM) over a colposcopic image sequence was proposed by Liang et al. where the specular reflection was removed using a binary reflection map by a threshold and the segmentation was guided by three characteristics that determine the presence of abnormal cells: whiteness changes of metaplastic epithelia, morphological changes around precursor lesions, and changes of vascular regions.

In this work, a methodology capable to segment the colposcopic image sequences ignoring the noise is presented, in order to guide to the medical expert in the selection of the appropriate region to take a sample for the biopsy. This methodology consists of two steps mainly; in the first, a preprocessing of the colposcopic images was made, in order to delete as much noise as possible; with this process, the use of only one image (disadvantage of [7], [8]) and the preprocessing proposed in [9] were improved. Last step comprises the implementation of the active contour model using an evolutionary algorithm to improve the greedy search (limitation of [9]). The main motivation of this work is to improve the segmentation of the acetowhite reaction in the colposcopic image sequence to support the pre-diagnosis of the cervical cancer and decrease the mortality rate of this illness.

It is important to mention that, the active contour model and evolutionary programming were selected because their good performance, fast convergence and easy implementation. Moreover, active contour model encircles all kinds of objects without a previous training phase, unlike other segmentation algorithms. Meanwhile, evolutionary programming algorithm does not restrict the length of individuals, being this a fundamental aspect to be considered for the design of the addressed problem.

A comparison among our methodology, other segmentation approaches and the expert appreciation were made to evaluate the performance and efficacy of our proposal. Two different segmentation approaches (using one image or a greedy search) were included to prove that our version is more competitive avoiding the undesired region. Results show that our methodology is a feasible and competitive tool to be implemented in the health area.

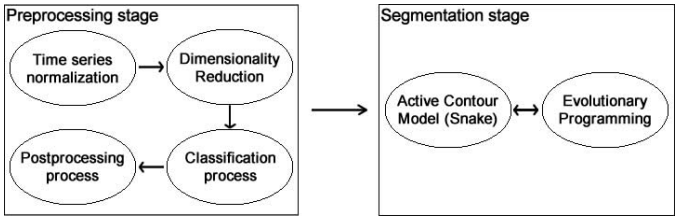

Fig. 1. Proposed methodology to segment cervical images.

The organization of this document is structured as follows: Section II describes our methodology to segment the cervical images, including the preprocessing done to reduce the noise in digital images and the segmentation algorithm used. Section III presents the experiment and results carried out to validate the viability of the proposed tool. Finally, in Sections IV and V, some discussions, conclusions and future work are presented.

II. Proposed Methodology

In this section, our proposed methodology is introduced. Figure 1 shows all included process in our methodology and the steps done in each process.

A. Preprocessing stage

Before mentioning each step in this stage, it is necessary to explain how the colposcopic images were obtained and their characteristics.

1) Colposcopic Images: The colposcopic test was performed using a DFV Vasconsellos CP-M7 colposcope with 16x magnification without optical filters. The focal distance between the cervix and the colposcope was 20 cm and the view radius was approximately 13 cm. Digital images were captured using a Sony SSC-DC50A and digitizer Matrox Meteor-II / Standard managed by an HP workstation xw6000 model running with Matlab 7.0. In the first ten seconds of the colposcopic test, ten images were captured at a rate of one frame per second (we will refer to this set of images as *reference images*); after that, another 300 images of the behavior of the acetic acid were obtained for five minutes using the same sample frequency [11].

This study involved 38 patients in total, selecting only 12 colposcopic image sequences for the experiment. This selection was based on the incidence of each type of noise as well as the presence of the acetowhite reaction. Each patient agreed to share their results to be used in this research.

2) Time series normalization: As aforementioned, one of the problems to be solved before implementing the proposal described is the reduction of significant noise on digital images captured. To reach this goal, it was necessary to change the color space of colposcopic images to a gray scale for an easier manipulation.

Afterwards, in order to analyze the behavior of the tonality of each region of the images, the time series for each pixel

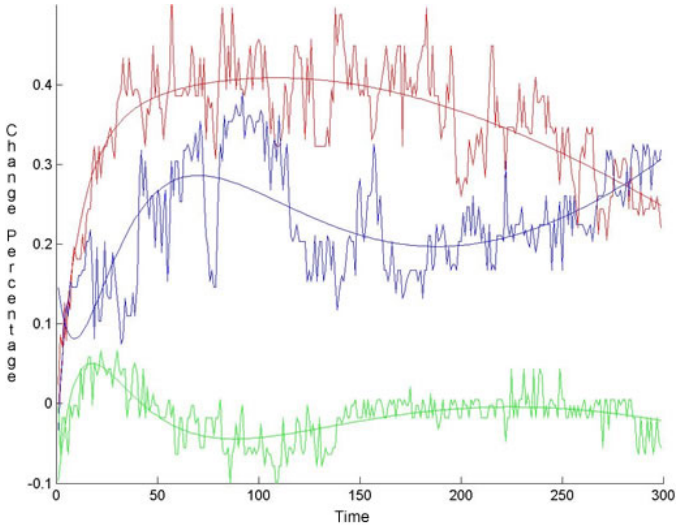

Fig. 2. Time series approximation with PCA model. The solid line represents the time series obtained from this model.

was extracted. Each time series presents different frequencies of shades, thus a normalization process was necessary. This process consisted in use the reference images to move every time series at one same frequency.

3) Dimensionality reduction: Even with the normalized time series, the computational cost to try to identify the noise in colposcopic images was still quite high. Hence, a reduction of dimensionality was computed. Hernandez-Galicia in [12] proposed two models to reduce the time series using fewer parameters: the polynomial model and Principal Component Analysis (PCA), the latter was selected for several reasons: 1) it can reduce high dimensional data (four variable for our case), 2) it can handle noisy, and 3) it can handle correlated data keeping most of the variance of the original data. However, the PCA method assumes static processes over dynamic processes under normal operating conditions and is only suitable for use in static conditions [13]. Figure 2 shows the similarity between the original time series and the adjusted time series by the PCA model (continuous line).

4) Classification process: One way to identify and discriminate noise in colposcopic images is applying a classification process. For this process, it was necessary to create a database with manually selected time series based on the behavior of all time series. Figure 3 shows several kinds of time series (specular reflection, keratosis and acetowhite reaction). At this point, we will refer to the acetowhite time series as Acetowhite response function (AWRF) [9].

A total of 1080 time series with 540 instances per each kind of time series per patient was selected. That is, 45 *AWRF's* and 45 time series where the acetowhite reaction is not presented were selected per each patient. As a consequence the database was balanced. The database attributes were the variables obtained by PCA model; the attribute class was the time series type, labelling as 1 for the *AWRF* and 2 for the noise time series.

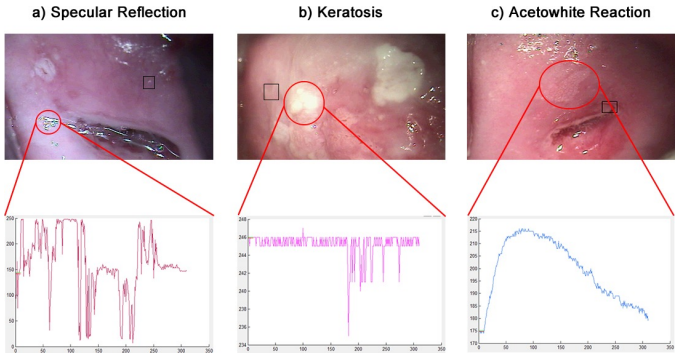

Fig. 3. a) Time series of specular reflection, b) Time series of keratosis and c) AWRF.

Subsequently, four different classifiers were applied to choose the one with the best performance in terms of accuracy, sensitivity and specificity. The selected classifiers were NaiveBayes, J48, k-NN and MultiLayer Perceptron (Neural Net). The latter was implemented in Matlab because it got the best results compared with others. As a result, a binary image with *AWRF's* was created.

5) Postprocessing process: As shown in table I, MultiLayer Perceptron (Neural Net) outperformed to 80% at media values in each indicator. However, it did not achieve reach a 100% in all indicators, so, approximately, a 10% of error range is presented. As a result, binary images with some noise included were obtained. Hence, a post-processing of the binary images was performed, using morphological operators to decrease the extra noise. The morphological operators used were *Dilation*, *Erosion*, *Opening* and *Closing*. *Dilation* consists in increasing or expanding a given object by a structuring element, and it is expressed in Equation 1, where A is the binary image, B is the structuring element, $\widehat{B}_z$ is the reflection of B about its origin and changed by the point z. In other words, the dilation of A by B is the set of all displacements (z) such that $\widehat{B}$ and A overlap by at least one element [14].

Erosion is the inverse operation of dilation. It seeks to reduce the pixel number of an object and it is expressed in Equation 2, where A is the binary image and B is the structuring element. Given this equation, the erosion is defined as the set of all points z such that B (moved by the point z) is part of A [14].

$$A \oplus B = \{z|([\widehat{B})_z \cap A] \subseteq A\} \tag{1}$$

$$A \ominus B == \{z|(B)_z \subseteq A\} \tag{2}$$

The *Opening* and *Closing* operations are combinations of the previous operators. Both try to soften the contour of an object. The first one removes small gaps between two portions of the object (Equation 3). Meanwhile, the closing operator links these portions, deleting bridges and, filling empty holes (Equation 4) [14].

Patient	Naive Bayes			J48			k-NN			MultiLayerPerceptron (Neural Net)		
	A	**Se**	**Sp**	**A**	**Se**	**Sp**	**A**	**Se**	**Sp**	**A**	**Se**	**Sp**
1	50.00%	100.00%	0.00%	78.89%	62.22%	95.56%	**85.56%**	**71.11%**	**100.00%**	71.11%	42.22%	100.00%
2	55.56%	100.00%	11.11%	86.67%	84.44%	88.89%	86.67%	80.00%	93.33%	**90.00%**	**100.00%**	**80.00%**
3	42.22%	84.44%	0.00%	40.00%	20.00%	60.00%	65.56%	40.00%	91.11%	**87.78%**	**75.56%**	**100.00%**
4	66.67%	71.11%	62.22%	75.56%	95.56%	55.56%	77.78%	88.89%	66.67%	**78.89%**	**95.56%**	**62.22%**
5	63.33%	91.11%	35.56%	85.56%	71.11%	100.00%	88.89%	77.78%	100.00%	**97.78%**	**95.56%**	**100.00%**
6	57.78%	100.00%	15.56%	75.56%	97.78%	53.33%	74.44%	100.00%	48.89%	**80.00%**	**100.00%**	**60.00%**
7	26.67%	24.44%	28.89%	46.67%	26.67%	66.67%	57.78%	35.56%	80.00%	**83.33%**	**80.00%**	**86.67%**
8	50.00%	100.00%	0.00%	86.67%	80.00%	93.33%	81.11%	71.11%	91.11%	**97.78%**	**100.00%**	**95.56%**
9	80.00%	66.67%	93.33%	68.89%	37.78%	100.00%	71.11%	44.44%	97.78%	**91.11%**	**82.22%**	**100.00%**
10	56.67%	91.11%	22.22%	97.78%	100.00%	95.56%	96.67%	100.00%	93.33%	**100.00%**	**100.00%**	**100.00%**
11	81.11%	88.89%	73.33%	84.44%	95.56%	73.33%	91.11%	91.11%	91.11%	**92.22%**	**93.33%**	**91.11%**
12	94.44%	100.00%	88.89%	92.22%	93.33%	91.11%	91.11%	88.89%	93.33%	**97.78%**	**100.00%**	**95.56%**
X	60.37%	84.81%	35.93%	76.57%	72.04%	81.11%	80.65%	74.07%	87.22%	**88.98%**	**88.70%**	**89.26%**

TABLE I

CLASSIFICATION RESULTS OF NOISE AND AWRF, WHERE THE ACCURACY (A), SENSITIVITY (SE) AND SPECIFICITY (SP) OF EACH CLASSIFIER IN THE 12 PATIENTS ARE INDICATED; THE AVERAGE OF EVERY ALGORITHM IS SHOWN AT THE TABLE BOTTOM. BOLD NUMBERS INDICATE THE BEST RESULTS OBTAINED FOR EACH PATIENT.

$$A \circ B = (A \ominus B) \oplus B \tag{3}$$

$$A \cdot B = (A \oplus B) \ominus B \tag{4}$$

The opening and closing operators were applied to the binary image generated by the neural network. A square was used as structuring element for each one with a size of 3 pixels for opening operator and 12 pixels for closing operator. The final binary image is shown in Figure 4.

Finally, with the binary image post-processed, the colposcopic image sequence was filtered to eliminate zones not classified as *AWRF*.

B. Segmentation process

1) Active contour model (Snake): Williams et al. in [15] proposed a fast convergence algorithm to optimize the segmentation of the original algorithm called *active contour model or Snake* introduced by Kass et al. in [16]. An active contour is a system of points connected one by one, where internal and external energies interact to find the minimum total energy of the system and thereby encircle an interest object; each of these points is called *control point (CP)* [9]. In other words, a Snake is a set of springs connected one by one, to surround an object in an image. Those springs will contract by releasing energy (internal energy), stopping when the object is encircled or when such release is completed. At the same time, object walls will release a repulsive force (external energy) to prevent the springs deform its shape [9].

The Equation 5 represents the entire system aforementioned, where s is the set of control points of the contour, E_{cont} represents the continuity energy which control the spring shape. E_{curv} represents the curvature energy that controls the stretching or bending of the springs. Both correspond to the internal energy of the system. E_{img} represents the image forces that control the resistance of the object to be perforated by the Snake (external energy). α, β and γ are user-defined weights to control the behavior of each energy.

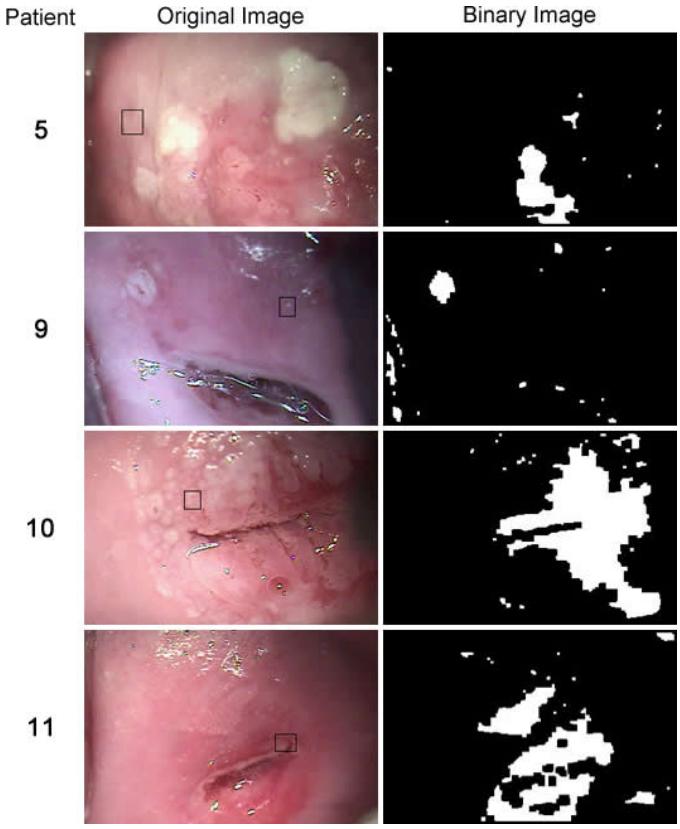

Fig. 4. Binarization results of colposcopic images using a neural network classifier on four different patients. The images on the left correspond to the original image, meanwhile, the images on the right correspond to the post-processed binary image with the morphological operators (opening and closing). The white regions on the binary images represent zones with acetowhite patterns and the black regions represent otherwise.

$$E = \int (\alpha(s)E_{cont} + \beta(s)E_{curv} + \gamma(s)E_{img})\, ds \tag{5}$$

In Equation 6, continuity energy was calculated. It was obtained from the difference between the average of all the

CP distances and the distance between the current (v_I) and previous point (v_{I-1}). This to avoid large gaps between each point [15]. Likewise, curvature energy was computed by obtaining the distances among the previous (v_{I-1}), current (v_I) and next point (v_{i+1}), as shown in Equation 7.

$$E_{cont} = |\bar{d} - (v_i - v_{i-1})| \tag{6}$$

$$E_{curv} = |v_{i-1} - 2v_i + v_{i+1}|^2 \tag{7}$$

Finally, external energy was calculated based on the gradient magnitude (Equation 8). The gradient calculation is a spatial operation to find edges or contours of an object into an image (G_x and G_y). That is, it allows to find differences in tonalities among pixel by using *kernels* or windows that are applied throughout the image by a matrix multiplication. Equation 9 illustrates the calculation of gradients for the x axis and for y axis, where the expression $\frac{\partial f}{\partial x}$ calculates horizontal edges of objects and the expression $\frac{\partial f}{\partial y}$ calculates vertical edges. Importantly, a contour is a discontinuity or abrupt change in the tone of a pixel with respect to its neighbors [9].

$$\bigtriangledown f = mag(\bigtriangledown f) = \sqrt{G_x^2 + G_y^2} \tag{8}$$

$$\bigtriangledown f = \begin{bmatrix} G_x \\ G_y \end{bmatrix} = \begin{bmatrix} \frac{\partial f}{\partial x} \\ \\ \frac{\partial f}{\partial y} \end{bmatrix} \tag{9}$$

$$G_x = \begin{bmatrix} -1 & 0 & 1 \\ -2 & 0 & 2 \\ -1 & 0 & 1 \end{bmatrix} G_y = \begin{bmatrix} 1 & 2 & 1 \\ 0 & 0 & 0 \\ -1 & -2 & -1 \end{bmatrix} \tag{10}$$

The fast algorithm aforementioned was implemented to find the acetowhite patterns in the colposcopic image sequence. Two modifications to the algorithm were done. First, the gradient calculation was readjusted by calculating the differences between the time series and their neighbors. Euclidean distance was used for this purpose. Equation 11 shown this modification, where ST_x and ST_y are the current time series and ST_{x+1} and ST_{y+1} are their neighbors. To compute the differences in the neighborhood of a pixel, Sobel mask was used. Last, in order to improve the algorithm performance, the stop condition was modified. It consisted in to define a threshold to decide if the algorithm could decrease the Snake total energy, counting the number of attempts done; if the threshold was exceeded and the energy has not been reduced, it is assumed that the algorithm has found a solution.

$$\begin{aligned} Gx &= \sqrt{TS_x^2 - TS_{x+1}^2} \\ Gy &= \sqrt{TS_y^2 - TS_{y+1}^2} \end{aligned} \tag{11}$$

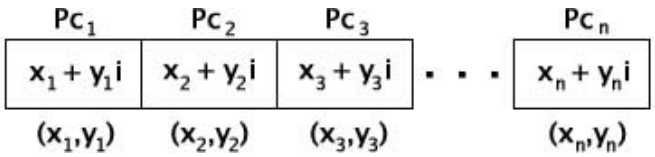

Fig. 5. Encoding of individuals based on the control points (CP) given by coordinates x and y.

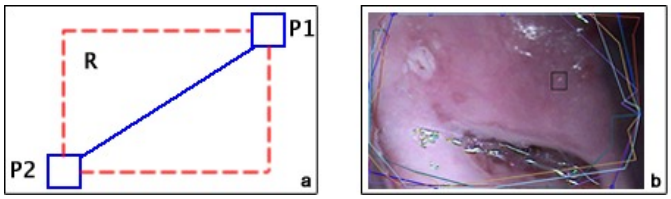

Fig. 6. (a) Solutions generation given the region R which is created by the control points P_1 and P_2; this area is the space where the new points are generated; (b) Example of a population generated in an image.

2) Evolutionary Programming: Evolutionary programming (EP) is a meta-heuristic method based on the principle of survival of the fittest, proposed by Charles Darwin. It considers evolution at the species level, i.e., offspring is generated only through mutation because individuals of different species are unable to create offspring. At each generation (cycle of the algorithm) each individual generates one offspring by mutation. Therefore, the size of the population increases. Due to that, a replacement mechanism takes place by using random encounters based on fitness. After that, the individuals with most wins in such encounters (from the union of the current population and all the offspring) will remain for the next generation and the rest of them are eliminated. The EP is one of the simplest evolutionary algorithms because no parent selection nor crossover operators are required.

The EP was used as part of the search mechanism of the Snake; encoding the individual of the population as a set of coordinates x and y into a vector using imaginary numbers, in order to apply the mutation operator in both values simultaneously; as shown in Figure 5. The initial population was generated inserting random points between the zone formed by each *CP* of the initial contour marked by the user; Figure 6 shown this process. The fitness function adopted by EP was the Snake general equation (Equation 5), which is a minimization function.

Three different mutation operators were designed to promote diversity in the population of solutions. The first one involved moving a control point to another location in the image, this displacement is executed within the area formed by the previous and next points of the current point, as shown in Figure 7(a). The second operator consisted in inserting a new point in the area given by the same points from the previous operator, see Figure 7(b); Finally, the third mutation consisted in removing the current control point and linking of the neighborhood points, see Figure 7(c).

The combination of these mutation operators makes that the Snake contour presents erratic behavior, i.e., big jumps

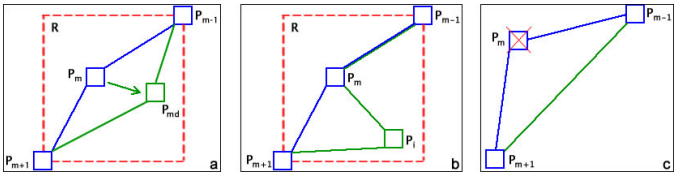

Fig. 7. Mutation operators used: (a) displacement, (b) insertion and (c) removal fo a control point.

Algorithm 1 Evolutionary programming algorithm

1: Create the randomly initial population using the representation of individual as shown in Figure 5 ;
2: Evaluate the generated population with the Equation 5;
3: **for** $i \leftarrow 1$ **to** number of generations **do**
4: Mutate every individual of the population with the operators described in Figure 7;
5: Evaluate the generated offspring in the previous step with the Equation 5;
6: Replace the population with the fittest individuals.
7: **end for**

in each *CP* is presented, deforming the contour or losing the direction towards the target. Therefore, it was necessary to control these movements by applying penalties to reward or punish those contours with undesired forms. The first penalty was based on counting the number of *AWRF's* in the area surrounding the Snake; the individuals with the highest number of *AWRF's* were rewarded and those with the shortest number were punished. Equation 12 expresses this penalty, where P_F represents the number of *AWRF's* and P_F^C is the complement of P_F, i.e., the number of time series that are not *AWRF*.

The second penalty is related to the existence of intersection points on some sides of the Snake contour. This penalty was computed by punishing the solutions with one or more intersections, increasing its fitness value with a very large value (10000 units). Equation 13 expresses this calculation, where $Inters(s)$ is a function to compute the number of intersections in the contour of the individual.

$$Pe_{area} = P_F^c - P_F \tag{12}$$

$$Pe_{inters} = \begin{Bmatrix} 0 & \text{Si} & Inter(s) = 0 \\ 10000 & \text{if} & Inters(s) \geqslant 1 \end{Bmatrix} \tag{13}$$

The replacement of solutions after the reproduction phase (each solution generates one offspring) was carried out by tournament selection. The proposed algorithm is described in the Algorithm 1.

III. Results

Experiments were designed to evaluate the usability and efficiency of our methodology (*Dynamic Evolutionary Snake (DES)*) in the medical field. For this reason, a comparison between the results obtained by our proposal and the manual segmentation of the expert. Before that, another comparison was carried out between two variants of our proposal, 1) *Dynamic Greedy Snake, DGS*, where the search mechanism is changed by a greedy heuristic, but using the same preprocessing stage, and 2) *Static Greedy Snake, SGS*, where only one image is used in computing the gradient based on the Equation 9.

The parameter setting used to execute DES, DGS and SGS, was defined as follows. The number of executions performed was five executions per patient with a population of 200 individuals, iterating on 300 generations. The mutation rate used was 80, generating one offspring for each individual in the population. The values of the weights for the Snake algorithm were calibrated by previous experiments where the values of $alpha = 1.5$, $beta = 1.2$ and $gamma = 9$ got better results.

Figure 8 shows the final contours found by every segmentation approach in four representative patients. The contour manually defined by the expert was included to visually validate the efficacy of each variant.

Furthermore, in Table II, the statistical indicators as the accuracy, sensitivity and specificity for each variant are summarized. Each statistic was estimated based on the manual contour by the expert. In other words, the manual contour of the expert was used as training data, while the contours obtained by each Snake variant were used as test data.

IV. Discussion

From the results presented in the previous section, a better performance of DES respect to SGS and DGS was observed. DES found areas with the highest concentration of *AWRF's* and got final contours consistent with expectations. Thus, the EP is a significant and important element in the task of avoiding undesired areas of the colposcopic images; although, it was helped by a preprocessing stage, we should not belittle the fact that the global search outperforms results search greedy.

In order to validate the independence of the algorithm with respect to the initial contour, an initial contour around the entire image was generated. DES was able to converge to the region of interest, avoiding all types of noises and demonstrating that it can even work without an initial contour, unlike the proposals presented in [7] and [9], where the initial contour played an important role in finding a good solution.

Regarding with the manual segmentation of the specialist, DES reached similar contours to those provided by the expert. Figure 8 and Table II demonstrate this asseveration, where SGS and DGS got good specificity values, but low values in accuracy and sensitivity. This because the contour of the expert (and external areas) was totally covered by the resulting contour of these Snakes, throwing false positives in prediction. In contrast, DES obtained better percentages in each estimator, showing the similarity with the contour provided by the expert.

It is worth mentioning that DES not coincided with two out of twelve patients with the manual contour provided by the colposcopist. In the first case (Patient 10 from Figure 8), the failure was because the manual area marked by the expert did

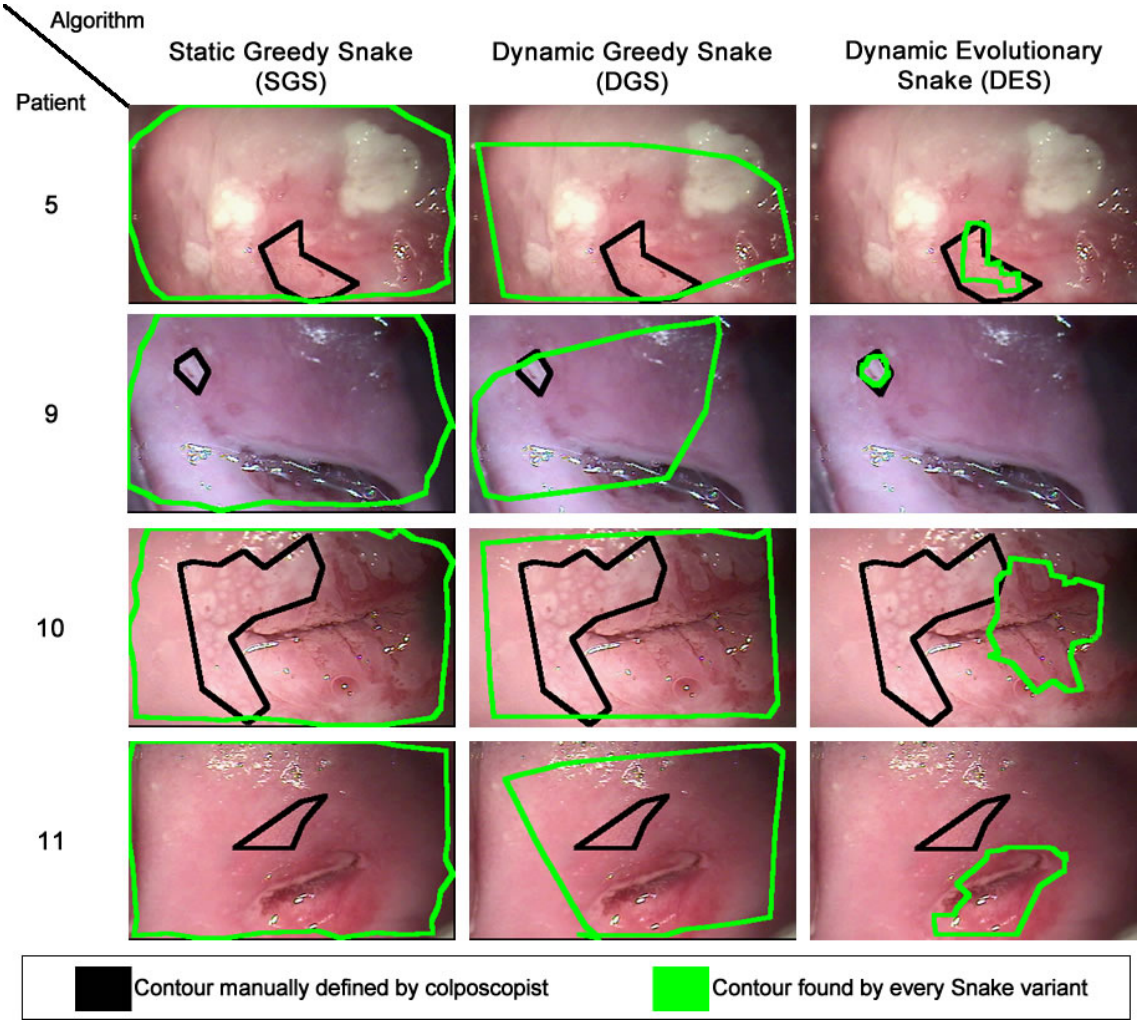

Fig. 8. Results found by every segmentation approach. a contrast between our approach and the manual contour defined by the colposcopist was made.

Patient	***SGS***			***DGS***			***DES***		
	A	**Se**	**Sp**	**A**	**Se**	**Sp**	**A**	**Se**	**Sp**
1	19.91	11.65	98.72	82.65	38.03	**99.93**	**91.61**	**57.37**	97.86
2	19.70	13.83	**100.00**	60.98	24.82	**100.00**	**82.04**	**41.35**	98.91
3	17.93	9.17	**100.00**	70.36	21.56	99.69	**92.93**	**82.26**	93.14
4	51.63	39.43	**92.11**	60.64	44.17	87.46	**67.68**	**49.59**	73.03
5	14.56	5.94	**100.00**	41.92	8.40	99.77	**96.83**	**88.54**	97.08
6	13.67	5.01	**100.00**	26.04	5.79	**100.00**	**97.51**	**75.77**	98.41
7	21.95	14.41	**100.00**	24.71	14.86	**100.00**	**92.67**	**77.54**	94.46
8	44.63	25.79	**100.00**	68.84	38.17	**100.00**	**91.74**	**75.69**	96.10
9	13.09	1.34	**100.00**	51.77	2.17	99.77	**99.62**	**97.95**	99.64
10	27.16	20.71	**99.48**	39.23	**23.80**	99.46	**65.41**	0.49	77.49
11	9.17	2.88	**100.00**	39.64	**4.27**	**100.00**	**86.71**	0.00	96.99
12	30.25	22.23	98.67	50.74	28.84	**99.62**	**94.34**	**80.79**	98.46
$\bar{x}$	21.82	13.26	**91.46**	47.50	19.61	91.21	**81.47**	**55.95**	86.27

TABLE II
SENSITIVITY (SE), SPECIFICITY (SP) AND ACCURACY (A) VALUES OBTAINED FOR EACH ALGORITHM VERSION WITH RESPECT TO THE MANUAL SEGMENTATION OF THE EXPERT.

not present changes in tonality in all the colposcopic image sequence, being classified as noise by the classification process and therefore, being discarded by the DES. For this patient, the expert selected this area watching other features used to assess whether the area is a possible injury to the cervix, but he did not discard the contour suggested by our algorithm. In the second case (Patient 11 from Figure 8), both contours contain similar amounts of *AWRF's*, being the contour found by DES

the solution with the lowest energy, according to the Equation 5, but in the opinion of the expert, any contour presented is a good sample to the biopsy.

V. Conclusions and future work

A methodology to segment colposcopic images was presented, using a preprocessing step and coupling the active contours method and evolutionary programming. The aim of the method was to improve the capabilities of the active contour method by adding it a global search algorithm instead the Greedy search considered in the original method in order to develop a support tool for the early detection of cervical cancer. Three mutation operators were designed to generate competitive Snakes based on the original energy-based quality value used in the segmentation method.

An experiment applied on twelve patients was carried out in order to analyze the performance of the proposed methodology. The results indicate that the proposed methodology is able to find the expected regions, avoiding noise present in the colposcopic images. Nevertheless, the two Greedy variants were trapped by such information. Furthermore, in ten out of twelve patients, the selected region was similar that the selected by the colposcopist. Finally, the accuracy, sensitivity and specificity values obtained by the proposed approach outperformed those obtained by the two Greedy Snake variants. In conclusion, our proposal is a competitive tool able to support to the colposcopist in the early detection of cervical cancer, becoming one more piece to decrease the mortality rate of this disease.

As a continuation of this work, we suggest adding features not addressed in this research regarding the properties of cervical lesions that can be listed as carcinogenic, to provide a better sensitivity and breadth of search to the segmentation algorithm. Additionally, it is necessary that DES finds more than one solution (with similar concentrations of *AWRF's*) in one execution, being the expert who decides the best sample for biopsy. Furthermore, we propose to implement an automatic calibration of the weights that control the behavior of the active contour algorithm, being part of the individual in the Evolutionary Programming algorithm. Finally, we suggest a lesion classification stage when one solution is found, classifying it according to lesion degree.

Acknowledgement

The first author thanks the Mexican National Council of Science and Technology through a scholarship to pursue graduate studies. The second author acknowledges support to CONACyT through the research grant: Fondo Sectorial de Investigacin en Salud y Seguridad Social SSA/IMSS/ISSSTE-CONACyT (Id:Health-2008-C01-86566).

References

[1] W. H. Organization, "New guidance for the prevention and control of cervical cancer." [Online]. Available: http://www.who.int

[2] Y. Tern-Figuero, P. Muiz-Carren, M. Fernndez-Moya, S. Galn-Cuevas, N. Noyola-Range, S. O. Gutirrez-Enrquez, J. Ortiz-Valdez, and A. Cruz-Valdez, "Repercusiones del cancer cervicouterino en pacientes con limitaciones de acceso a los servicios de salud," *Ginecol Obstet Mex*, vol. 83, no. 3, pp. 162–172, 2015.

[3] K. Duraisamy, K. Jaganathan, and J. Chandra Bose, "Methods of detecting cervical cancer," *Advances in Biological Research*, vol. 5, no. 4, pp. 226–232, 2011.

[4] B. Apgar, M. Spitzer, and G. Brotzman, *Colposcopía. Principios y práctica + DVD-ROM: Manual y atlas integrados*. Elsevier Health Sciences Spain, 2011.

[5] B. W. Pogue, H. B. Kaufman, A. Zelenchuk, W. Harper, G. C. Burke, E. E. Burke, and D. M. Harper, "Analysis of acetic acid-induced whitening of high-grade squamous intraepithelial lesions," *Journal of Biomedical Optics*, vol. 6, no. 4, pp. 397–403, 2001.

[6] B. C., "A novel optical imaging method for the early detection, quantitative grading, and mapping of cancerous and precancerous lesions of cervix," *IEEE Transactions in Biomedical Engineering*, no. 48, pp. 96–104, 2001.

[7] V. Van Raad and A. Bradley, "Active contour model based segmentation of colposcopy images of cervix uteri using gaussian pyramids," in *Proceeding 6th International Symposium on Digital Signal Processing for Communication Systems (DSPCS'02)*, 2002.

[8] K. Nallaperumal and K. Krishnaveni, "Watershed segmentation of cervical images using multiscale morphological gradient and hsi color space," *International Journal of Imaging Science and Engineering (IJISE)*, vol. 2, no. 2, 2008.

[9] H. G. Acosta Mesa, R. Hernández Jiménez, K. Gutiérrez Fragoso, and A. J. Magallanes Lugo, "Segmentación de lesiones cérvico uterinas aplicando contornos activos sobre patrones espacio temporales," in *V. Congreso Latinoamericano de Ingeniera Biomédica CLAIB 2011*, La Habana, Cuba, Mayo 2011.

[10] M. Liang, G. Zheng, X. Huang, G. Milledge, and A. Tokuta, "Identification of abnormal cervical regions from colposcopy image sequences," 2013.

[11] H. G. Acosta Mesa, N. Cruz Ramírez, and R. Hernández Jiménez, "Aceto-white temporal pattern classification using k-nn to identify precancerous cervical lesion in colposcopic images," *Computers in Biology and Medicine*, vol. 39, no. 9, pp. 778–784, Septiembre 2009.

[12] E. Hernández Galicia, "Propuesta metodológica para la detección de lesiones precursoras del cáncer cérvico uterino utilizando funciones dinámicas de respuesta acetoblanca," Master's thesis, Departamento de Inteligencia Artificial de la Universidad Veracruzana, 2006.

[13] D. Bogle, I. Bogle, and M. Fairweather, *22nd European Symposium on Computer Aided Process Engineering*, ser. Computer-Aided Chemical Engineering. Elsevier Science Limited, 2012. [Online]. Available: https://books.google.com.mx/books?id=qDToVTz84roC

[14] R. Gonzalez and E. Woods, *Digital Image Processing*, 2nd ed. Prentice-Hall, 2002.

[15] D. Williams and M. Shah, "A fast algorithm for active contours and curvature estimation," *CVGIP: Image Underst.*, vol. 55, no. 1, pp. 14–26, Jan. 1992.

[16] M. Kass, A. Witkin, and D. Terzopoulos, "Snakes: Active contour models," *International Journal Of Computer Vision*, vol. 1, no. 4, pp. 321–331, 1988.